

LA-5170-PR

PROGRESS REPORT

0.3

CIC-14 REPORT COLLECTION
**REPRODUCTION
COPY**

Performance of Multiple HEPA Filters
Against Plutonium Aerosols

for Period July 1 through December 31, 1972

LOS ALAMOS NATIONAL LABORATORY
3 9338 00402 3882



los alamos
scientific laboratory
of the University of California
LOS ALAMOS, NEW MEXICO 87544

UNITED STATES
ATOMIC ENERGY COMMISSION
CONTRACT W-7405-ENG. 36

This report presents the status of the Performance of Multiple HEPA Filters Against Plutonium Aerosols at LASL. The previous quarterly in this series, unclassified, is:

LA-5012-PR

In the interest of prompt distribution, this progress report was not edited by the Technical Information staff.

Printed in the United States of America. Available from
National Technical Information Service
U. S. Department of Commerce
5285 Port Royal Road
Springfield, Virginia 22151
Price: Printed Copy \$3.00; Microfiche \$0.95

LA-5170-PR
Progress Report
UC-41

ISSUED: January 1973



Los Alamos
scientific laboratory
of the University of California
LOS ALAMOS, NEW MEXICO 87544

Performance of Multiple HEPA Filters Against Plutonium Aerosols

for Period July 1 through December 31, 1972

by

Harry J. Ettinger, Project Manager
John C. Elder
Manuel Gonzales



PERFORMANCE OF MULTIPLE HEPA FILTERS AGAINST PLUTONIUM AEROSOLS

by

Harry J. Ettinger, Project Manager, John C. Elder, and Manuel Gonzales

ABSTRACT

The field sampling program has been completed at four of the five original locations in three AEC plutonium processing plants. Size characteristics have been defined in terms of aerosol activity median aerodynamic diameter (amad) and geometric standard deviation (σ_g) using the Andersen eight-stage impactor. While size parameters show day to day variations, these can generally be classified within sufficiently narrow limits to permit development of typical criteria. Three locations yielded amad ranging from 0.9 to 4.0 μm ; σ_g , from 1.5 to 4.0. The remaining site exhibited much higher activity concentrations and smaller amad (0.1 to 1.0 μm).

The laboratory experimental system to test multiple HEPA filters has been assembled. Its design will permit definition of series filter efficiency as a function of particle size using plutonium aerosols closely approximating those defined by the field sampling program. Initial tests of an aerosol generator which nebulizes a water suspension of ball-milled ^{238}Pu resulted in an aerosol amad of 0.85 μm , σ_g of 2.4, and activity concentration of 8×10^{10} dpm/ m^3 . Selective ball-milling of the bulk powder, addition of anionic surfactant to the suspension, and ultrasonic agitation of the suspension provide control of size characteristics over the range of interest.

Calculations to evaluate the possibility of ^{238}Pu particles being sufficiently hot to damage the HEPA filter glass fibers indicate surface temperatures for ^{238}Pu particles under 150 μm amad much lower than the softening point of borosilicate glass fibers in HEPA filters.

I. SUMMARY

Sampling has been completed at four of five original locations in three AEC plutonium processing plants. One sampling location remains active after relocation to a point in the process ventilation system which contains higher plutonium aerosol concentrations. While size characteristics and activity concentrations are variable in all locations, as would be expected from

the wide variety of processes in each plant, a high percentage of the activity median aerodynamic diameter (amad), geometric standard deviation (σ_g), and activity concentration falls within limits sufficiently narrow to permit development of typical criteria. Size characteristics for Locations 00, 04, and 14 were obtained from Andersen impactor data operating at the normal 1.0

cfm flow rate. Results for Location 11 were obtained by operating the Andersen impactor at 2.75 cfm to permit definition of aerosol size characteristics down to 0.1 μm . At Locations 00, 04, and 14 the ranges of source term aerosol characteristics were similar, with an amad range of 0.9 to 4.0 μm ; σ_g range of 1.5 to 4.0; and activity concentrations ranging from 10^3 to 10^5 dpm/ m^3 . Sampling data show activity at Location 11 to be several orders of magnitude higher than at any other facility (10^6 to 10^7 dpm/ m^3), with an aerosol amad varying from 0.1 to 1.0 μm .

Additional consideration was directed at the potential problems associated with deterioration of impactor surfaces; impactor operation at various barometric pressures; particle rebound; and wall losses at the higher (2.75 cfm) impactor flow rate. Based on experimental data and theoretical considerations the potential errors associated with these sampling variables are not significant.

The laboratory test system has been installed at the test area and is operational. Modification of the ReTec X-70/N nebulizer provides an aerosol generator with increased output, which when used in an array of six yields activity concentration of $\sim 10^{11}$ dpm/ m^3 . To facilitate counting impactor samples of this relatively large activity concentration upstream of the first filter, a dilution system was developed. The Nuclepore filter sampling activity concentration at this location is dissolved in chloroform and diluted for counting. Particle size characteristics of a $^{238}\text{PuO}_2$ powder ball-milled for 360 hours are amad = 0.85 μm and $\sigma_g = 2.38$. This distribution approximates the smallest Pu aerosol size distribution measured at three field sampling locations.

Heat transfer calculations were performed to investigate the possibility that particles of high specific activity material, such as ^{238}Pu , become hot enough to damage glass filter fibers, thereby causing

a significant decrease in filter efficiency. Using a simplified model, and assuming ^{238}Pu particles do not exceed an amad of 150 μm , these calculations indicate surface temperatures to be much lower than the softening point of borosilicate glass fibers used in HEPA filters. Heat removal by either conduction or radiation can limit surface temperature of particles small enough to be found on HEPA filters to only a few $^\circ\text{C}$ above ambient. Heat removal by convection to the air in motion past the particle probably has even greater influence over surface temperatures. These estimates indicate that high specific activity particles are not capable of damaging filter fibers by raising fiber temperature to the softening point. The only exception would be for HEPA filters located at a glove box which may collect extremely large particles which are not capable of airborne transport for any significant distance.

II. FIELD SAMPLING

A. Background

Three AEC plutonium processing plants (LASL, Mound, and Rocky Flats) were selected as suitable field sampling sites, representative of many research and production operations utilizing both ^{238}Pu and ^{239}Pu . Five sampling locations, two each at Mound and Rocky Flats and one at LASL, have been monitored immediately upstream of the exhaust HEPA filters using Andersen impactors for particle size analysis and membrane filters for activity concentration. Typical sampling procedures called for one daily sample during the most active periods of the working day, or when activity concentrations could be expected to approximate "worst normal" conditions. The wide variety of plant operations and amounts of material handled produced variable particle size characteristics and activity concentrations. Another variable was better filter performance at some glove box locations. Although the variability of particle size characteristics and activity concentration

complicate data handling, useful generalizations can be made regarding typical aerosols incident on exhaust HEPA filters to provide criteria for generating similar aerosols in the laboratory.

The sampling techniques chosen initially have proven adequate for this program. The Andersen impactor has sufficient range to measure particle size characteristics at all locations. Its operation is simple so that valid samples were obtained without extensive training and close supervision of personnel taking the samples. Sample handling and shipping to a central point for analysis has proceeded without difficulty. Cooperation by local personnel has been satisfactory and only in one case,

at Location 08, has major delay been encountered, due primarily to low priority assigned to relocating a sampling location to another duct in the same building. Currently, Location 08 is the only active sampling location of the original five.

B. Results and Discussion

1. Aerosol Size Characteristics.

Size characteristics based on alpha activity measurements of particles deposited on impactor stages for Locations 00, 04, 11, and 14 are summarized in Table I and graphically displayed as frequency histograms normalized to percent of total observations in Fig. 1-4. As in the last progress report,¹ particle size characteristics are expressed as activity median aerodynamic

TABLE I

SUMMARY OF SIZE CHARACTERISTICS AND ACTIVITY CONCENTRATIONS OF PLUTONIUM AEROSOLS

Activity median aerodynamic diameter (amad)			
At Location __,	__%	of __ observations	fall in the range __ μ m to __ μ m
00	94	94	0.9 to 2.7
04	66	32	1.0 to 4.0
11	90	19	0.1 to 1.0
14	92	51	1.5 to 3.2

Geometric standard deviation (σ_g)			
At Location __,	__%	of __ observations	fall in the range __ to __
00	93	94	1.5 to 3.0
04	81	32	2.0 to 3.3
11	63	19	2.2 to 4.4
14	88	51	2.0 to 4.0

Activity Concentration (A)			
At Location __,	__%	of __ observations	fall in the range __ to __dpm/m ³
00	87	77	10 ³ - 10 ⁵
04	72	46	10 ³ - 10 ⁵
11	88	57	10 ⁶ - 10 ⁷
14	75	56	10 ⁴ - 10 ⁶

diameter (amad) and geometric standard deviation (σ_g) determined by non-linear least-squares fit of cumulative grouped data (percent of total alpha activity less than indicated diameter versus effective cutoff diameters of impactor stages). All data were assumed to follow a log normal size distribution. Although this assumption is not always correct (to be discussed later), the method is convenient and provides consistent approximation of the aerosol size characteristics. An alternate method of data analysis is being investigated. The choice of amad over several other statistical representations of size (mass median aerodynamic diameter, mass median diameter, or count median diameter)² was based on several conditions: (1) amad is most meaningful in studying filtration of radioactive particles since the variable of concern is how much activity in a certain particle size range arrives at or passes through a filter, and (2) aerodynamic diameter best defines particle-filtration mechanism in the size range of interest (0.1 μm to 5 μm microscopic diameter).

Table I indicates that plutonium aerosol size characteristics at three of four locations are similar with an amad range of 0.9 to 4.0 μm and σ_g range of 1.5 to 4.0. At the fourth site the aerosol is much smaller with an amad range of 0.1 to 1.0 μm . Figure 1 represents amad and σ_g as normalized frequency histograms, along with activity concentration in histogram form, for Location 00, a facility in which a wide variety of research and development activities are performed using both ^{238}Pu and ^{239}Pu . From the histograms, the following statements regarding amad and σ_g can be made:

94% of amad 's were observed between 0.9 μm and 2.7 μm , and

93% of σ_g 's were observed between 1.5 and 3.0.

Figure 2 summarizes similar data for Location 04, a research-development facility

dealing primarily with ^{238}Pu . At Location 04:

66% of all amad 's were observed in the range 1.0 μm to 4.0 μm , and

81% of all σ_g were observed between 2.0 and 3.3.

It may be noted that amad 's for Location 04 show greater variation than results from other locations.

Figure 3 summarizes the data from Location 11, a recovery facility handling ^{239}Pu . This location was the source of an unusually small aerosol requiring operation of the Andersen impactor at 2.75 cfm to lower the effective range of particle collection. Some amad 's and σ_g 's for Location 11 were determined visually from log probability graphs since the computer fit program had not been altered to accommodate the new impactor cutoff diameters for operation at 2.75 cfm. The results will be re-analyzed by the computer fit method at a later date. At Location 11:

90% of amad 's were observed between 0.1 μm and 1.0 μm , and

63% of σ_g 's were observed between 2.2 and 4.4.

Size characteristics for Location 14 are presented in Fig. 4. Location 14 samples process ventilation from ^{239}Pu machining and fabrication activities. Size characteristics at this location generally are consistent with other locations except Location 11. At Location 14:

92% of amad 's were observed between 1.5 μm and 3.2 μm , and

88% of σ_g 's were observed between 2.0 and 4.0.

Size characteristics for Location 08 are being measured after relocation of the sampling site downstream of its original location. The new location includes a third glove box line which contributes significantly to the activity in this air-stream.

2. Activity Concentrations. Table I summarizes variations in activity concentration at each location. Histograms

providing detail are included in Figs. 1, 2, 3, and 4. Consistently high concentrations (10^6 to 10^7 dpm/m³) are noted at Location 11, which is located in one of several ducts discharging into a single plenum.

3. Spectrometry. Alpha spectrum analysis of impactor samples from Location 00 (the only location handling both ²³⁸Pu and ²³⁹Pu) detected day-to-day variation in isotopic ratios on each impactor stage. Although *amad* is a valid parameter to describe the size characteristics of the composite distribution, the relationship between *amad* of the composite distribution and *amad* of each isotopic distribution was not known. Several sets of impactor samples were analyzed by silicon surface barrier detectors coupled to a 400 channel spectrum analyzer. Activity of each isotope on each impactor stage was obtained by summing counts in analyzer channels under each peak of the spectrum and dividing by total counting time to yield the count rate for a specific energy range. Graphing the cumulative count rates (Fig. 5) provided the size characteristics for each isotopic distribution, and the sum of these two provided the composite distribution. Figure 5 shows significant difference between size characteristics of the two constituents, with *amad*'s of 1.7 μ m for ²³⁸Pu and 1.0 μ m for ²³⁹Pu. The *amad* of the isotope mixture lies between those two values.

Spectrum analysis also showed that particles collected on each type of impactor coating surface, including the DM 800 vinyl metricel finally selected as a coating material, caused negligible absorption of alpha particles. The evidence of low absorption was a minimal downward shift of ²³⁹Pu alpha peaks detected by silicon surface barrier detector looking at PuO₂ particles impacted on various coating materials. The following table summarizes channel shifts observed:

<u>Coating</u>	<u>Peak Shift</u>
Whatman 41	Channel 100 to Channel 85
DM 800 Vinyl	Channel 100 to Channel 85
Glass Fiber	Channel 100 to Channel 90

Glass fiber filter material showed least absorption; however, the other two materials were not sufficiently inferior to justify their exclusion in favor of a much thicker filter which would have unknown effect on impaction parameters due to grossly altered ratio defined by the jet-to-plate distance and jet diameter.

4. Filter Penetration. Downstream impactor and membrane filter (MF) data taken at Location 00 in the period May-June 1972 provided a limited amount of activity penetration data for these exhaust filters. Data analysis was hampered by low count rates on downstream samplers despite week-long sample runs. Filter penetration was calculated from MF samples by dividing average downstream concentration by the sum of upstream concentrations determined for the period when upstream and downstream samplers were operating simultaneously. Radical changes (sometimes improvement in efficiency) cast serious doubt over the accuracy of these measurements. These measurements were not considered sufficiently accurate for reporting in quantitative terms, but served to illustrate the difficulty of efficiency determinations based on gross activity. Future measurements should include the following: (1) inspection and correction of MF sampling stream, (2) larger sample size downstream, and (3) possible evaluation of efficiency in particle size ranges from upstream and downstream impactor data.

C. Experimental Apparatus and Techniques.

1. Size Separation by Andersen Impactor. The procedures and principles of operation of the Andersen impactor, the primary size selective sampler utilized in the program, were covered in detail in the previous progress report. Since that time effort was expended in three areas related to operation of the impactor: (1) particle rebound evaluation, (2) calibration of the impactor at atmospheric pressure other than the manufacturer's sea level calibration, and (3) calibration of the

impactor at flows significantly higher than maximum flow recommended by the manufacturer. The latter effort was directed at lowering the cutoff diameters for each stage to characterize the smaller aerosol at Location 11, a recovery facility. The following discussion covers details of experiments and calculations aimed at enhancing confidence in size characteristics measurements.

a. Particle Rebound Evaluation.

Due to several cases of particle rebound cited in the literature,^{3,4} the possibility of extensive rebound in the Andersen

impactor has been considered in three ways: (1) the impaction plates have been coated with filter media to reduce rebound as suggested by Knuth,⁴ (2) all impactor data have been reviewed for evidence of rebound as manifested in large amounts of activity on the backup membrane filter or downward shift of σ_{g} , and (3) dual impactors, one with coated plates and the other uncoated, were operated simultaneously to detect possible signs of rebound. Table II contains size characteristics in categories of impaction surface for all locations. These data reflect the arithmetic averages

TABLE II

ANDERSEN IMPACTOR AT 1.0 CFM
SIZE CHARACTERISTICS OF Pu AEROSOL

Description	Location	#Obs	amad (μ m)			σ_g		
			Mean	Max	Min	Mean	Max	Min
No coating	00	77	1.75	3.94	.43	2.31	4.50	1.53
AA ^a	00	10	1.86	2.70	.92	2.38	2.85	1.83
DM 800 ^b	00	7	1.91	2.50	1.25	2.22	3.32	1.74
All samples	00	94	1.78	3.94	.43	2.31	4.50	1.53
DM 800	04	8	3.12	5.51	1.26	2.79	4.70	2.01
WH41 ^c	04	17	3.19	11.55	.23	2.86	6.33	2.03
No coating	04	7	2.43	5.76	.23	2.61	3.75	2.07
All samples	04	32	3.01	11.55	.23	2.88	6.33	2.01
DM 800	08	9	2.25	2.99	1.35	2.28	2.71	1.88
DM 800	11 ^e	14	.30	.67	.12	5.17	10.8	2.58
Type E ^d	11 ^e	5	1.00	2.28	.09	4.77	10.4	2.13
All samples	11 ^e	19	.48	2.28	.09	5.07	10.8	2.13
No coating	14	11	2.37	3.53	1.53	3.10	6.40	1.98
AA	14	10	2.41	3.25	1.61	3.02	6.61	2.06
DM 800	14	30	2.51	8.60	.96	3.18	6.95	2.00
All samples	14	51	2.46	8.60	.96	3.13	6.95	1.98

^aAA - Millipore filters (0.8 μ m pore size)

^bDM 800 - Gelman vinyl metrical filters (0.8 μ m pore size)

^cWH41 - Whatman 41

^dType E - Gelman glass fiber filters

^eSample flow 2.75 cfm this location only

and extremes of σ_{amad} and σ_g . Although arithmetic average is not always the most precise parameter of data distribution, it would show any significant differences in σ_{amad} or σ_g which might be attributable to particle rebound. As noted in earlier reports, the coatings applied to the plates appear to have little effect on the consistency of results, even at 2.75 cfm flow rate. Although the mean of σ_{amad} 's determined with data from an impactor coated with Type E glass fiber filter is larger in Table II than similar data with DM 800 filter media, it was noted that the Type E values were influenced by a single high σ_{amad} and should not be considered a strong indication of particle rebound.

One week's samples from dual impactors (discussed in the last progress report) were consistent and revealed (1) no significant downward displacement of median diameter measured on the uncoated plates or (2) no unusually heavy deposit on the backup filter. Another week's data collected subsequently did not show evidence of rebound but variations between impactors indicated a major difference in the sampling streams. Interference between the probe tips or slight misdirection of probes during impactor handling is suspected. Further sampling of this type was not considered worthwhile in the absence of significant indication of rebound.

b. Effect of Atmospheric Pressure On Impactor Calibration. The impactor manufacturer provided a calibration performed at sea level atmospheric pressure. Three of our five sampling locations are located above 6,000 feet elevation. Calculations were performed to evaluate the effect of a roughly 25% decrease in atmospheric pressure.

Impaction theory is described by the equation:⁵

$$\psi_{s_0} = \frac{4 C(P, D_{s_0}) \rho P_i Q_a D_{s_0}^2}{18 \pi \eta D_j^3 P_0 N} \quad (1)$$

where ψ_{s_0} is a dimensionless impaction parameter

D_{s_0} is a physical diameter at 50% collection efficiency (cm)

$C(P, D_{s_0})$ is Cunningham slip correction at pressure P and diameter D_{s_0}

ρ is particle density (g/cm^3)

P_i is pressure at the inlet to the jet (cm Hg)

P_0 is pressure at the outlet of the jet (cm Hg)

Q_a is total flow ($\frac{cm^3}{sec}$)

η is viscosity of air at outlet of the jet ($\frac{g}{sec-cm}$)

D_j is diameter of the jet (cm)

N is number of jets in the stage.

Assuming the impaction parameter ψ_{s_0} is constant for round jets regardless of location or conditions, constants in equation (1) (η, ρ, Q_a, N, D_j) can be cancelled and the following expression relating sampling variables under different ambient pressures derived:

$$\frac{D'_{s_0}}{D_{s_0}} = \left[\frac{P_i}{P_i} \frac{C}{C'} \frac{P_0}{P_0} \right]^{1/2} \quad (2)$$

where D'_{s_0} and other primed parameters are related to calibration conditions at sea level while the unprimed parameters represent conditions at the sampling site. Pressure upstream and downstream of each jet stage, P_i and P_0 , were measured directly by manometer in the laboratory while maintaining total flow Q_a at 1.0 cfm (Los Alamos conditions). Slip corrections C and C' were calculated by the equation (3):

$$C = 1 + \frac{0.01}{P_0 D} \left[1.23 + 0.41 \exp(-86 pD) \right]$$

where P_0 is outlet pressure in mm Hg and D is particle physical diameter (cm) estimated from the original D'_{s_0} . The ratio D'_{s_0}/D_{s_0} ranged from 0.993 for Stage 0 to 0.960 for Stage 7, the latter value indicating a cutoff diameter 4% below the calibration value of 0.43 μm . The magnitude of this variation is small compared to the overall accuracy of measurement in this size range, and application of this minor correction to previous size data is not justified.

c. Effect of High Flows on Impactor

Calibration. Detection at Location 11 of an aerosol with size characteristics too small for evaluation with the Andersen impactor operated at 1.0 cfm led to investigation of higher sampling flow in the impactor as suggested by Hu.⁶ Higher sampling flow increases particle velocity and reduces pressure between stages, resulting in impaction of the particle on an earlier stage. Based on Hu's experimental results, Stage 6 cutoff diameter was expected to shift from 0.65 μm at 1.0 cfm, to 0.17 μm at 3.0 cfm. If particle rebound at the higher velocities can be controlled by application of filter media to the impaction surfaces, the impactor can be used to define aerosols with amad's as small as 0.1 μm .

Cutoff diameters were calculated to compare with Hu's experimental results and to compensate for an equipment-imposed flow limit of 2.75 cfm. Calculated values also provided cutoff diameters for Stages 0, 1, and 7 which were not obtained experimentally by Hu. The D_{50} of each stage was calculated by equation (1) using an impaction parameter $\psi = 0.10$ recommended by Mercer and Stafford.⁷ Inlet and outlet pressures, P_1 and P_0 , were experimentally determined by manometer readings upstream and downstream of each stage at the 3.0 cfm flow. The calculated and experimental values are compared in Table III. Since good agreement exists between calculated and experimental results in Table III, the calculated D_{50} for Stages 0, 1, and 7 provide adequate estimates of actual 50% cutoff diameters.

New stainless steel probes were prepared for isokinetic sampling at 2.75 cfm. Activity concentration samples were obtained as usual at 1.0 cfm using 47 mm membrane filter holder. Losses of particles on impactor walls and jet plates have been estimated for the 2.75 cfm flow rate by swipe tests of these surfaces and by experimental results reported by Hu. The swipe tests

TABLE III

CALCULATED CALIBRATION OF
ANDERSEN IMPACTOR
AT INCREASED FLOW

Effective Cutoff Diameters (D_{50}) in μm

Stage No.	Calculated		Experiment*
	2.75 cfm	3.0 cfm	3.0 cfm
0	7.67	7.35	-
1	3.54	3.39	-
2	2.40	2.30	2.4
3	1.61	1.54	1.5
4	1.00	0.96	0.9
5	0.46	0.44	0.4
6	0.23	0.22	0.17
7	0.12	0.12	-

*Hu's experimental values⁶

show activity collected on walls and jet plates of the first few stages to be less than 3% of the activity passing through these stages. The experimental results of Hu indicate losses up to 10% for polystyrene latex particles 0.23 and 0.36 μm , and practically no losses for larger particles (0.56 to 1.95 μm). These wall losses are a minor source of error and not large enough to warrant detailed study.

2. Sampling Locations. Of the five sampling locations at Los Alamos, Mound and Rocky Flats, sampling has been concluded at four Locations 00, 04, 11 and 14. The remaining location (Mound Laboratory) was relocated to include a duct carrying additional radioactive particles. The new location is still designated 08 and can be described as a production area.

Corrosion of an aluminum probe occurred at Location 04 (an r & d facility) to the extent that a minor force caused the probe to break as it was being removed from the duct at completion of sampling. The condition of the probe might have caused some change in sampling characteristics, although results from Location 04 give no

indication of a change. Future sampling probes should be constructed of stainless steel as required earlier at Location 11. Because of this experience with aluminum probes, the aluminum jet plates of the Andersen impactors have been inspected for corrosion or jet enlargement. No evidence of corrosion was observed. The impactors have remained in generally good condition. O-ring seals between stages were in good condition. Alpha contamination limits future use of the impactors except in cases where they can be cleaned externally and used locally for Pu particle sizing.

3. Data Analysis. In past reports size characteristics of all aerosols were reported as amad and σ_g on the assumption that particle sizes were lognormally distributed. Graphical representation indicates that many samples are not. In order to develop some criterion for accepting or rejecting an aerosol as being lognormally distributed, LASL Group C-5 aided in setting up a "goodness of fit" test incorporated in the computer nonlinear least squares fit program. The initial attempt, a chi-square test based on expected and observed numbers of particles, was not successful. The chi-square test becomes very powerful in detecting discrepancies in the distribution when high count rates (high numbers of particles) are observed. Even impactor data very carefully selected from a straight line plot on a log probability graph was rejected at the 90% probability level. Unless a rigorous statistical test for lognormality is developed, limiting deviation of any point from the best fit line to 10-15% may be an adequate test to reject data which should not be analyzed as lognormal. Another method which may prove useful and informative is presented for Location 11 in Fig. 6. The total activity in a size range (i.e., on the same impactor stage) for all observations is divided by total activity in all size ranges to provide a graph of percent of total activity as a function of particle

aerodynamic diameter. Cumulative percent of total activity as a function of aerodynamic diameter is presented in Fig. 7.

III. EXPERIMENTAL TEST PROGRAM

A. Experimental System

The laboratory test system has been constructed and installed in the test area. This system will permit testing three HEPA filters in series using plutonium test aerosols with size characteristics similar to those defined by the field sampling program. HEPA filter efficiency will be determined in terms of total activity passing each filter and as a function of plutonium aerosol size. The system is arranged in two modules: (1) a nine foot long glove box, housing the aerosol generating system, first stage HEPA filter and upstream samplers (Fig. 8), and (2) a hood connected at right angles to the glove box, housing the second and third stage test HEPA filters, associated samplers, and vacuum pumps (Fig. 9).

1. Plutonium Generation. Several plutonium aerosol generating methods were investigated and the choice for this study is a modified ReTec nebulizer⁸ (Fig. 10). Modification of this instrument entailed enlarging holes in the cap (Fig. 10, #5) and jet (Fig. 10, #6) to twice their original size. This resulted in a threefold increase in aerosol output, from ~ 300 $\mu\text{l}/\text{min}$ to ~ 900 $\mu\text{l}/\text{min}$ at 50 psig operating pressure. The generator solution reservoirs (Fig. 10, #1) were constructed of brass to a capacity of 70 ml to allow generation times up to one hour, O-ringed for elimination of leaks and Teflon coated to minimize wall losses. Using six of these nebulizers attached to a central duct (Fig. 11), with a generator solution concentration of 2.5 mg/ml $^{238}\text{PuO}_2$ suspended in water, should yield the plutonium aerosol concentrations required to test three HEPA filters in series.

To keep the suspension well stirred and achieve a constant aerosol output, the

reservoirs are partially immersed in an ultrasonic bath throughout the aerosol generation run. Because the aerosol is produced from a water suspension, care must be exercised to assure that all water is dried from the particles before arriving at the samplers and the first HEPA filter. The 25 cfm makeup air supplied to the system at room temperature did not accomplish complete drying. Supplying hot air at the system air inlet (Fig. 8, #2), raising the temperature of the system air about 10°C, did dry the aerosol.

2. Ball-Milling of $^{238}\text{PuO}_2$. To most closely approximate the plutonium aerosols present under field conditions, $^{238}\text{PuO}_2$ described as having a $2\ \mu\text{m} \pm 1\ \mu\text{m}$ mean physical diameter, was ball-milled 360 hours. A 250 mg sample of this ground powder was suspended in 100 ml water and stirred vigorously for 2 hours. A slide prepared from this suspension showed particle agglomerates ranging from 2 to 14 μm , with a small concentration of finer particles. A slide prepared from the clear supernatant after allowing the suspension to stand overnight showed most of the particles to be fine, well dispersed singlets. The relatively low particle concentration indicated that the larger agglomerates had settled to the bottom. A third slide prepared after the suspension was stirred and placed in an ultrasonic bath for one hour showed well dispersed individual particles with some agglomeration.

Addition of a small amount of "Dowfax 2A1" anionic surfactant solution and subsequent sonication for one hour showed very little agglomeration and a high concentration of discrete particles. The suspension with surfactant was allowed to stand over the weekend. No visual evidence of settling was observed as the solution remained homogeneously cloudy. The slide from this procedure showed the best dispersion with no agglomeration and a high particle concentration. These results indicate the benefits from ultrasonic

agitation to break up agglomerates, and from addition of an anionic surfactant to keep the particles well dispersed.

Extraction replication and electron microscope sizing of the above slide samples is not yet completed so we cannot yet report particle size characteristics of the suspended material by this method. By varying ball-milling time we should be able to modify particle size distributions to simulate those defined by the field sampling program.

3. Sampling and Sample Preparation.

a. Samplers. To obtain sufficient activity downstream of the third HEPA filter in series it was calculated that an activity concentration of $\sim 10^{12}$ dpm/m³ has to be produced by the aerosol generating system. This high activity level upstream of the first HEPA filter will result in activity levels on the first impactor which are virtually impossible to handle with the counting facilities available. To circumvent this problem, a sample dilution system was designed to draw a relatively small sample (.05 cfm) at the sampling probe, to be diluted with 0.95 cfm filtered air. To provide this 20:1 dilution and assure operation of the impactor at its design flow rate, an air line supplying 1.0 cfm to a mixing chamber (Fig. 8, #23) is split into two branches by a pair of rotameters, one a coarse branch (3 cfm capacity, Fig. 8, #26), and the other a fine branch (2 lpm capacity, Fig. 8, #25). Air is allowed to enter the chamber, 0.95 cfm through the coarse branch and 0.05 cfm through the fine branch, with the 1.0 cfm being drawn through the Andersen impactor. When the air flow is balanced as described above, the flow at the sampling probe is zero. By decreasing the flow through the fine rotameter from 0.05 cfm to zero, the resulting imbalance between supplied diluting air and flow through the Andersen impactor is made up by 0.05 cfm being drawn in at the sampling probe. Careful balancing, by means of a highly sensitive magnehelic gauge, and

air flow calibrations have yielded accurate flow and dilutions at the sampling probe.

Andersen impactors are also placed downstream of the first HEPA filter (Fig. 9) and second HEPA filter (Fig. 9). These will define the efficiency of each HEPA filter used in series, as well as efficiency as a function of particle size. These two size selective samplers will not need dilution systems because the activity concentration at those positions should be sufficiently low to permit counting.

A gross filter sampler will be used at each location, concurrently with the Andersen samplers, to monitor total aerosol concentration. These data will be used to determine overall HEPA filter efficiencies. Sampling times will vary for each sampling position with one minute being sufficient for position number one (upstream of first HEPA filter) and possibly one hour for position number three (downstream of second HEPA filter). With these gross differences in sampling times, it will be necessary to take several samples at position number one during each run to ascertain the variation in aerosol generator output as a function of time.

Due to the minimal amount of activity expected to penetrate all three HEPA filters, it is desirable to collect all plutonium at that point in the test system. A multiple, glass filter holder was designed for this purpose (Fig. 12). Filters from this apparatus as well as all filters and impactor plates from other samplers can be counted in our new counting facility.

b. Sample Preparation. Filters from the gross samplers upstream of the first HEPA filter as well as some of those used as anti-rebound agents on the Andersen impactor plates and the impactor backup filter may be too active to permit counting. These filters will be dissolved and diluted for counting. Nuclepore filters are readily soluble in chloroform, and the 0.8 μ m pore size Nuclepore filters were

tentatively selected for use since they have been recommended for sampling sub-micron aerosols.⁹ Performance of Nuclepore filters against a sub-micron plutonium aerosol will be evaluated. If necessary Millipore AA filters can be substituted, since these are soluble in acetone. All samples whether direct filter samples or diluted plated samples are wrapped in mylar film for counting.

B. Preliminary Aerosol Generation Test

To check generator output and aerosol particle size characteristics, the ball-milled $^{238}\text{PuO}_2$ which was sonicated after addition of surfactant was loaded into one generator while the other five generators were loaded with pure water. The Andersen sampler at position number one was turned on after generation had progressed for one minute. A one minute sample was collected with sample flow rate and diluting air flow rate as described previously. Andersen impactor plates and backup filter were counted and results plotted on log probability paper as the cumulative percent of activity less than a stated diameter, against the effective cutoff diameter assigned to that stage.^{1,10} Results of this first size test run (Fig. 13) showed the amad to be 0.85 μ m with a σ_g of 2.4. This particle size distribution approximates the smallest distribution seen at three field sampling locations.

Aerosol concentration measurements were taken for this test run also for one minute concurrently with the Andersen sampler. Results showed activity concentration challenging the first HEPA filter of:

$$7.815 \times 10^{10} \frac{\text{dpm}}{\text{m}^3}$$

at a system flow rate of 25 cfm.

C. Counting Facilities

The new alpha counting system described in the previous report¹ has been completed. It will be installed in a 30' x 10' mobile trailer which has been moved on site at the Occupational Health Laboratory building. Remodeling is almost complete and will

be ready to move into within a week or two. Final calibrations on the counting system will be done at that time.

IV. EFFECT OF HIGH SPECIFIC ACTIVITY PARTICLES ON HEPA FILTER MEDIA

A. Background

With the aid of LASL Group T-3, a theoretical investigation was made into the possibility of particles of high specific activity material such as ^{238}Pu being hot enough to damage glass filter fibers, thereby causing a significant decrease in filter efficiency. While not specifically concerned with the performance of multiple HEPA filters, this question is related to the overall problem of HEPA filter reliability in atmospheres containing material of this type.

The particulate material incident on exhaust HEPA filters probably does not exceed 50 μm physical diameter since this is comparable to an amad of 150 μm . Only in special cases such as a glove box HEPA filter located only a few feet from the source would particles exceeding 50 μm reach the filter. These special cases were not of primary interest. The particles of interest are the larger airborne particles of a high specific activity material dispersed into air, probably by some mechanical process in the recovery or production sequence. Background information in the following table was gathered from several sources^{11,12,13} to develop a realistic model.

Heat generation of ^{238}Pu : 0.56 watt/g
Particle density: 10.0 g/cm³
Particle diameter: 50 μm maximum
Fiber diameters: 70% 0.5-0.6 μm
30% 0.4-0.5 μm
Maximum interstitial distance
in a fiber mat: 15 μm
Fiber mat thickness: 0.020 cm
Borosilicate glass softening
temperature: 1254°F (677°C)
Borosilicate glass thermal
conductivity: 2.5×10^{-3} cal/cm/sec/°C

B. Calculations and Results

The heat transfer calculations detailed in Appendix indicate surface temperatures on ^{238}Pu particles to be much lower than the softening point of borosilicate glass used in HEPA filters. Heat removal by either conduction or radiation can limit surface temperature of particles small enough to be found on HEPA filters to only a few °C above ambient. Heat removal by convection to the air in motion past the particle probably has even greater influence over surface temperature. These estimates lead to the conclusion that high specific activity particles are not capable of damaging filter fibers by raising fiber temperature to the softening point.

V. FUTURE WORK

- A. Sampling with Andersen impactor and membrane filter upstream of exhaust filters at Location 08 will continue until a sufficient number of valid samples are collected.
- B. Upstream and downstream samples at Location 00 will be obtained for counting and spectroscopy analysis. Size characteristics upstream and downstream of a HEPA stage and filter efficiency in each impactor size interval will be studied.
- C. All HEPA test filters will be DOP pretested at LASL.
- D. Final testing of the aerosol generating system performance in different particle size ranges will be carried out.
- E. Multiple HEPA filter efficiencies against plutonium aerosols will be determined for several particle size distributions.
- F. Preliminary investigation (literature review) of other potential air cleaning systems for Pu processing plants will be initiated into some of the following areas:
 1. Sand filters
 2. Deep-bed filters
 3. Wet scrubbers

VI. ACKNOWLEDGMENT

The cooperation, guidance and assistance of the following people in completing the field sampling program and initiating the laboratory program are gratefully acknowledged:

E. J. Cox and W. L. Workman, H-1, LASL; D. G. Carfagno and W. H. Westendorf, Monsanto Research, Mound Lab; W. D. Kittinger and E. A. Putzier, Dow Chemical, Rocky Flats Plant; and C. E. Klatt and F. Miley, CMB-11, LASL.

VII. REFERENCES

1. H. J. Ettinger, J. C. Elder, and M. Gonzales, "Performance of Multiple HEPA Filters Against Plutonium Aerosols," LA-5012-PR (July 1972).
2. T. Hatch and S. P. Choate, *Journal of the Franklin Institute*, 207, 369-387 (1929).
3. G. W. Parker and H. Buchholz, "Size Classification of Submicron Particles By a Low Pressure Cascade Impactor," ORNL 4226 (June 1968).
4. R. Knuth, Health Protection Engineering Division, USAEC, NYOO, Private Communication (May 1972).
5. W. E. Ranz and J. B. Wong, "Jet Impactors For Determining The Particle Size Distributions of Aerosols," *Archives of Industrial Hygiene and Occupational Medicine*, 5, 464-477 (1952).
6. John Nan-Hai Hu, "An Improved Impactor for Aerosol Studies - A Modified Andersen Impactor," Ethyl Corp. report to be published in *Environmental Science and Technology*.
7. T. T. Mercer and R. G. Stafford, "Impaction from Round Jets," *Annals of Occupational Hygiene*, 12, 41-48 (1969).
8. *Manufacturer's Bulletin*, ReTec Development Laboratory, Portland, Oregon.
9. K. R. Spurny, J. P. Lodge, Jr., E. R. Frank, and D. C. Shiesley, "Aerosol Filtration by Means of Nuclepore Filters Aerosol Sampling and Measurement," *Environmental Science and Technology*, 3, 464-468 (May 1969).
10. T. T. Mercer, "On the Calibration of Cascade Impactors," *Annals of Occupational Hygiene*, 6, 1-14 (1963).
11. Dr. H. Knudsen, Hollingsworth and Voss Co., Private Communication (October 1972).
12. R. K. Jones, Johns-Manville Products Corp., Private Communication (October 1972).
13. H. Gilbert, USAEC-DOS, Private Communication (September 1972).

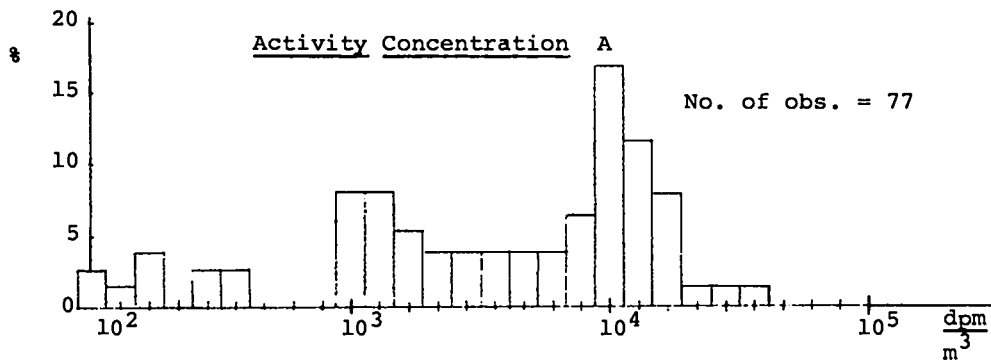
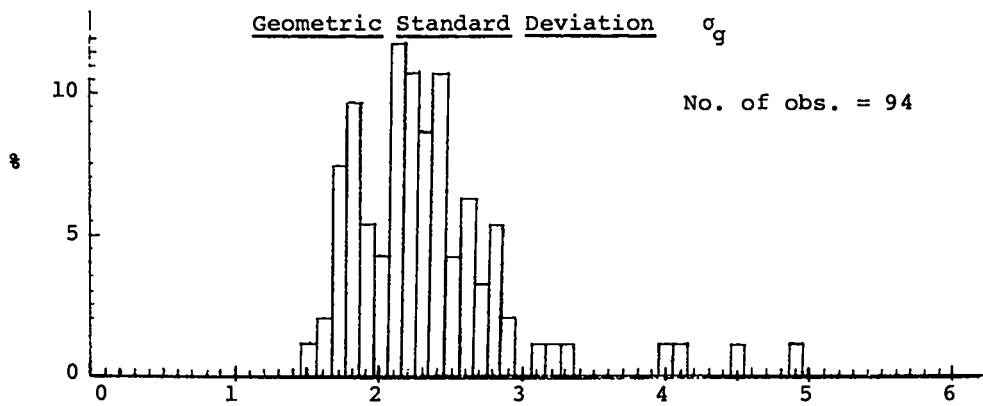
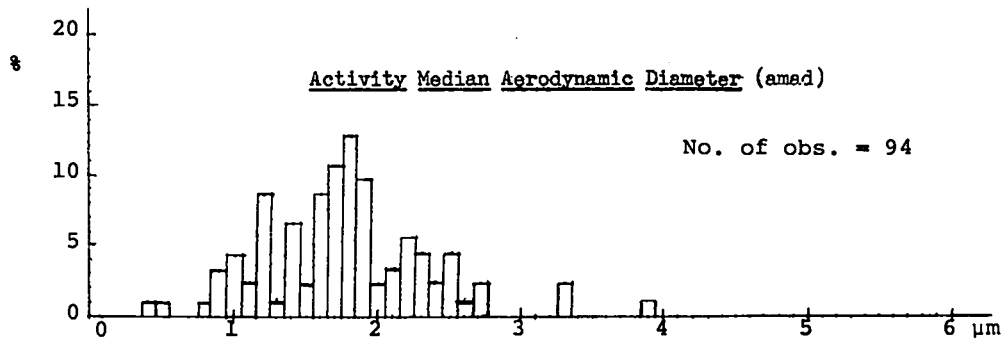


Figure 1: Frequency Histograms of amad , σ_g , and A at Location 00.

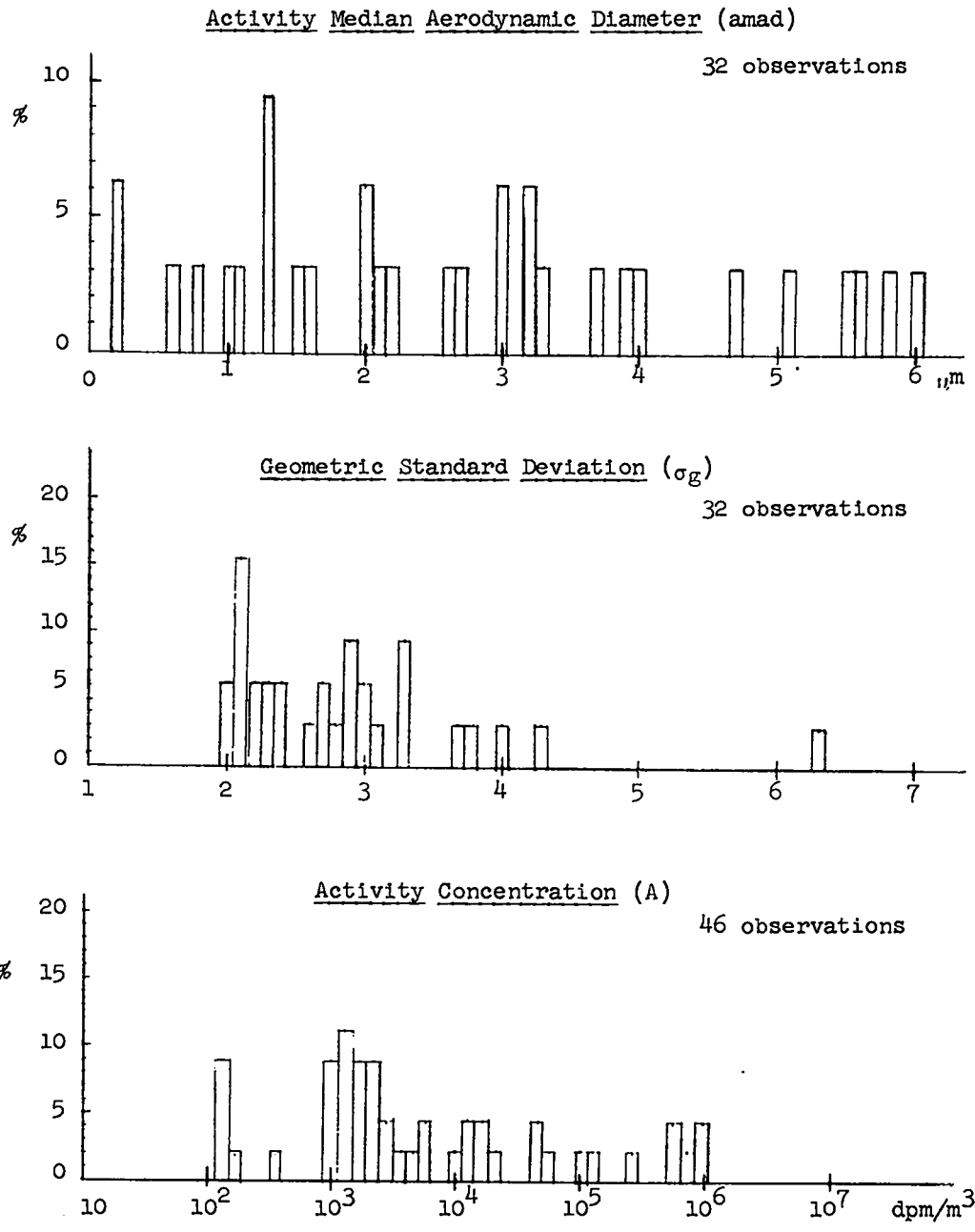


Figure 2: Frequency Histograms of amad, σ_g , and A at Location O4.

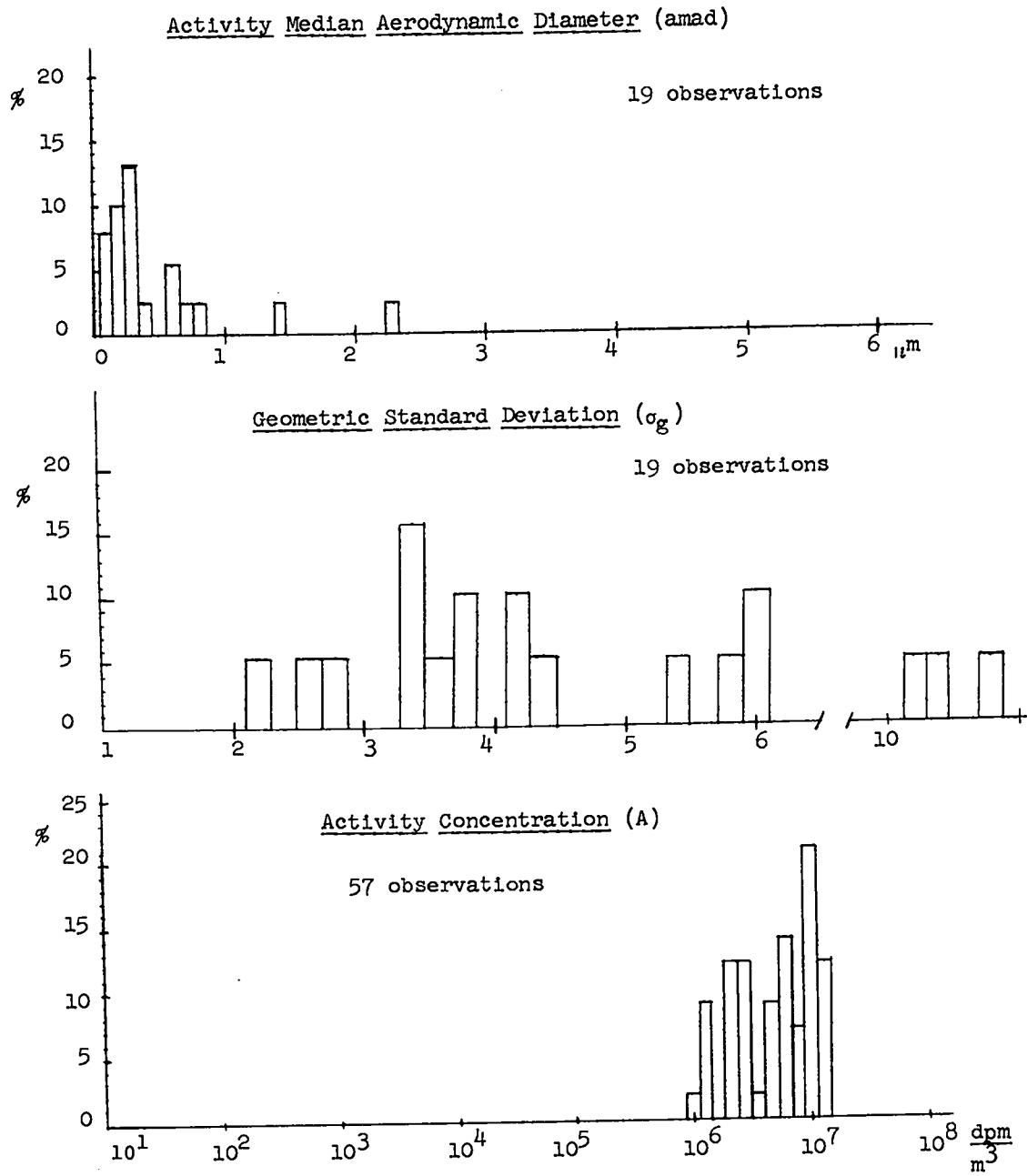


Figure 3: Frequency Histograms of amad, σ_g , and A at Location 11.

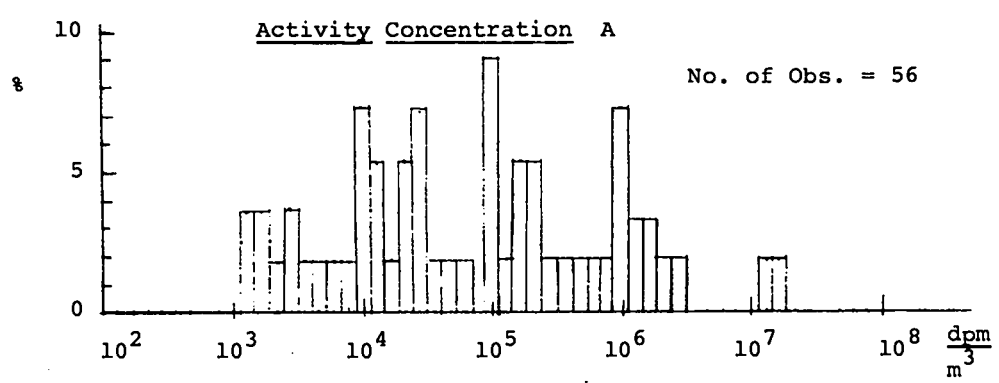
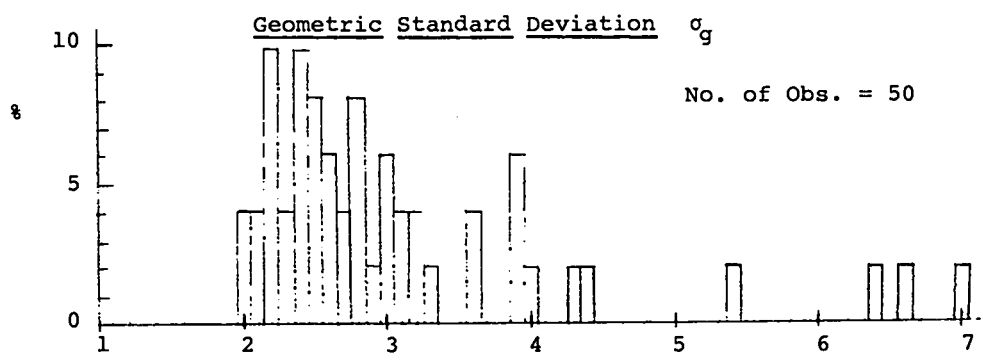
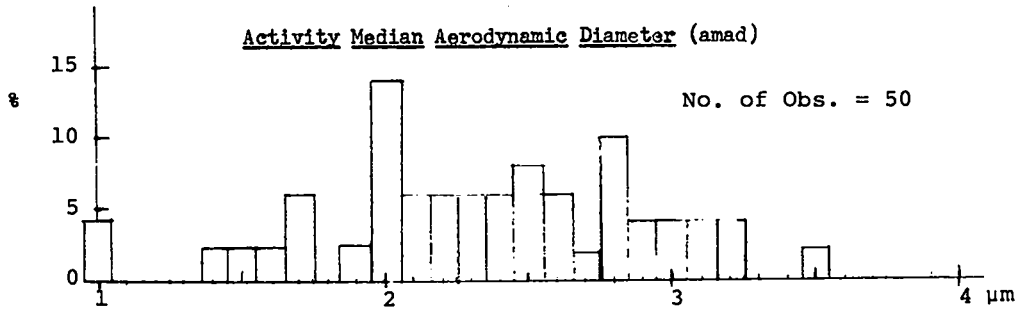


Figure 4: Frequency Histograms of amad , σ_g , and A at Location 14.

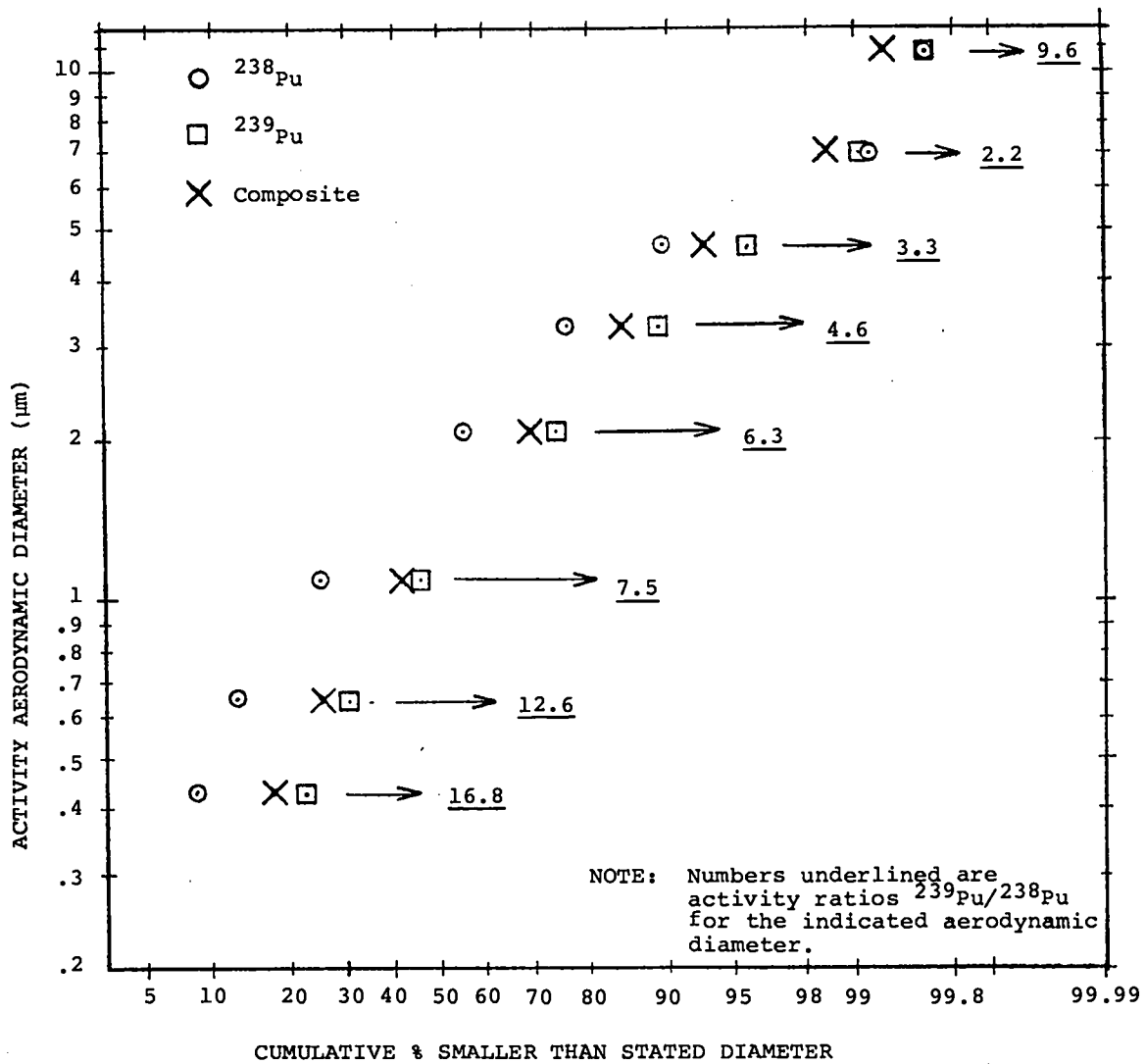


Fig. 5. Particle Size Characteristics Based on Spectrometry Results-- Location 00, May 22, 1972.

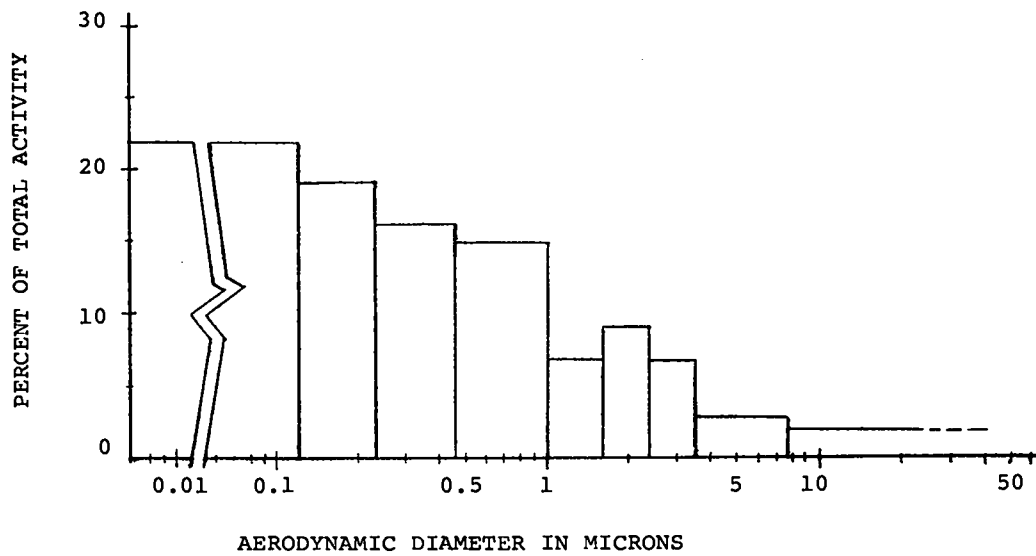


Fig. 6. Plutonium Aerosol Size Characteristics Based On All Samples at Location 11.

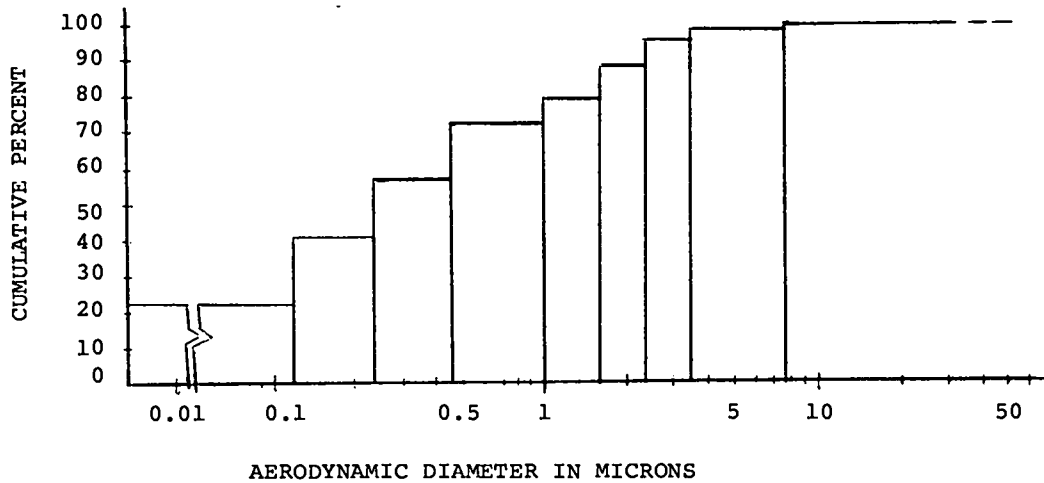


Fig. 7. Cumulative Display of Data In Figure 6.

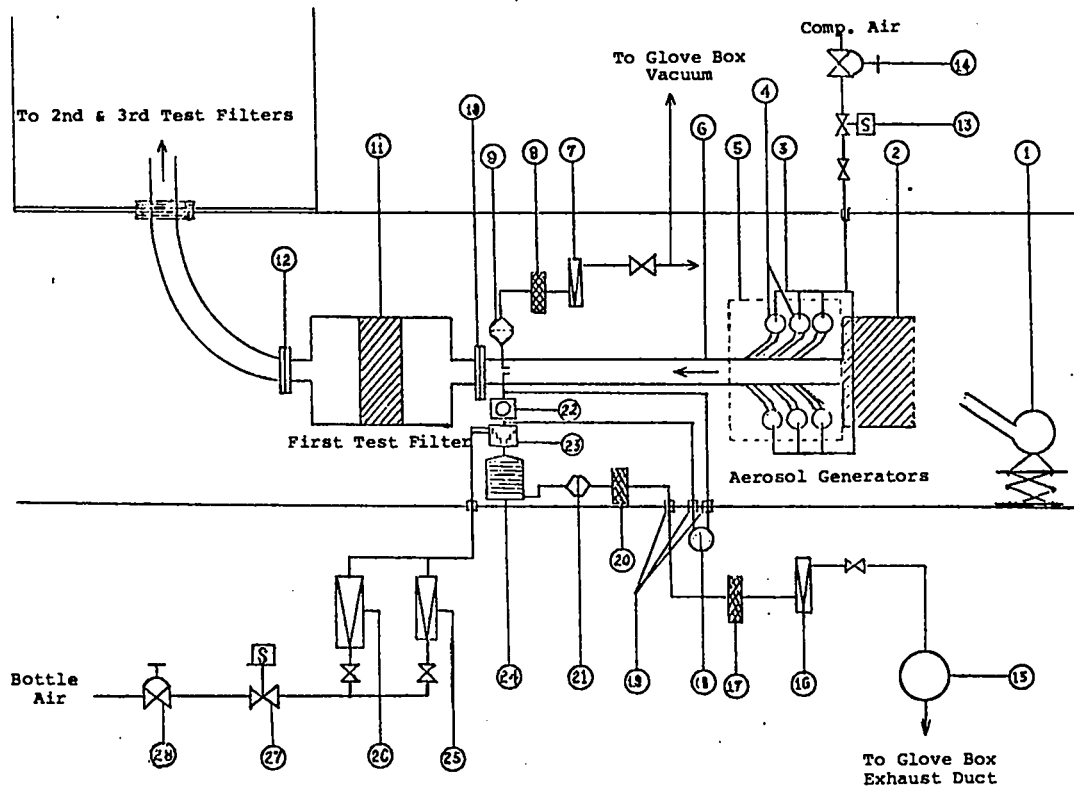


Fig. 8. Multiple HEPA Filter Test System - Module #1

REFERENCE NUMBERS FIGURE #8

1. Heat gun.
2. Intake air HEPA filter (open face).
3. Generator air supply manifold.
4. ReTec nebulizers.
5. Ultrasonic cleaner bath.
6. System duct 1-7/8" I.D.
7. Rotameter for Sampler #1.
8. MSA type H in-line filter.
9. Gelman 47 mm filter holder with filter.
10. "o"-ring sealed flanges.
11. HEPA test filter No. 1.
12. "o"-ring sealed flanges.
13. Safety interlock switch - generator air supply line.
14. Compressed air regulator.
15. Sampling vacuum pump.
16. Rotameter.
17. MSA type H in-line filter.
18. Magnehelic gauge.
19. Bulkhead fittings.
20. MSA type H in-line filter.
21. Gelman 47 mm filter holder with filter.
22. Ball valve.
23. Diluting chamber.
24. Andersen Impactor.
25. Rotameter-fine-flow balancing system for diluter.
26. Rotameter-coarse-flow balancing system for diluter.
27. Safety interlock switch-diluting air supply.
28. Compressed air regulator.

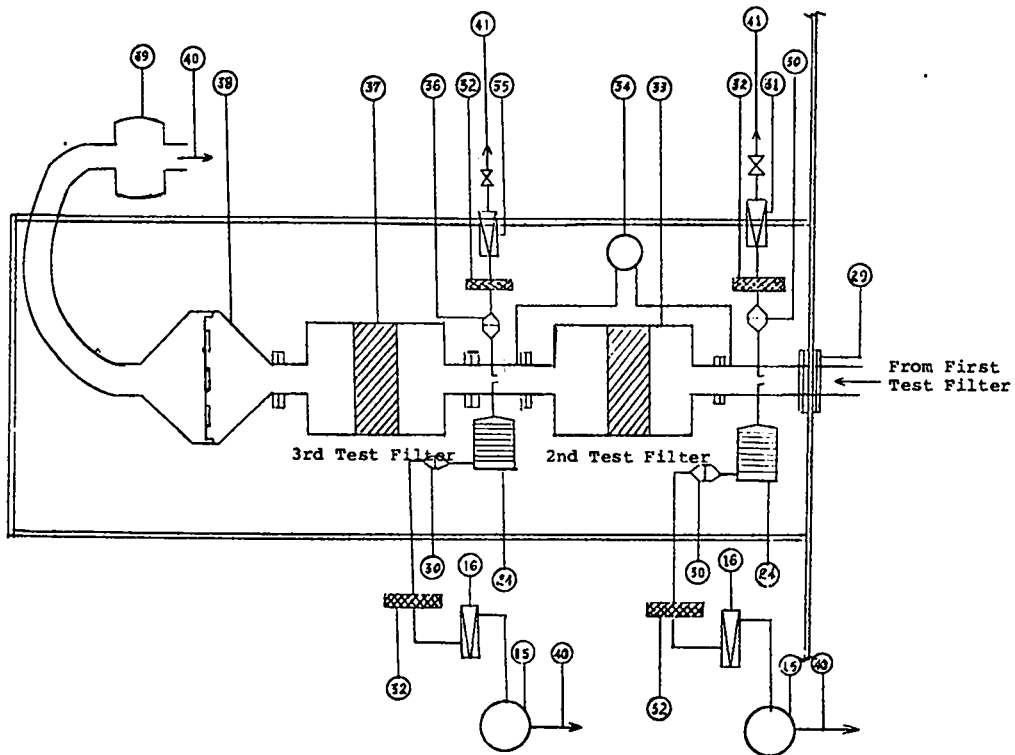


Fig. 9. Multiple HEPA Filter Test System - Module #2

REFERENCE NUMBERS FIGURE #9

- 29. "o"-ring sealed flanges - glove box to hood.
- 30. Gelman 47mm filter holder with filter for sampler No. 2.
- 31. Rotameter for sampler No. 2.
- 32. MSA type H in-line filter.
- 33. HEPA test filter No. 2.
- 34. Magnetohelic gauge for system flow calibration.
- 35. Rotameter for sampler No. 3.
- 36. Gelman 47mm filter holder with filter for sampler No. 3.
- 37. HEPA test filter No. 3.
- 38. Multiple filter sampler for sampler No. 4.
- 39. System vacuum pump.
- 40. To hood ventilation duct.
- 41. To hood vacuum.

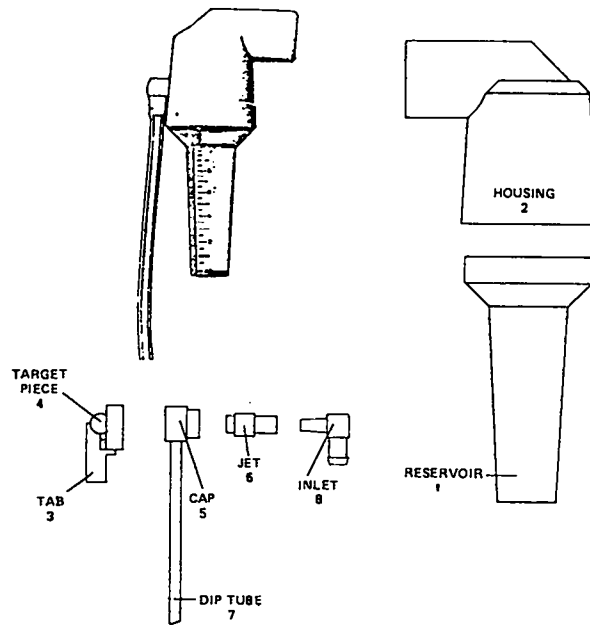


Fig. 10. ReTec X-70/N Nebulizer

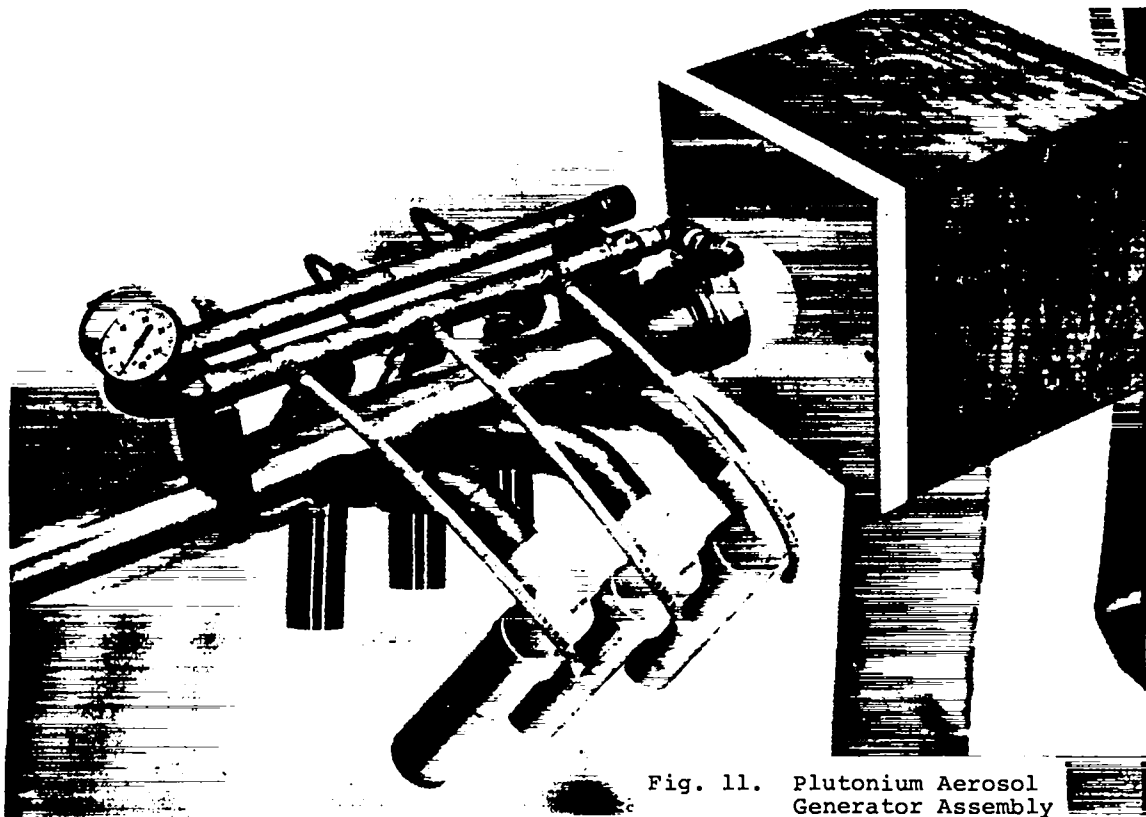


Fig. 11. Plutonium Aerosol Generator Assembly

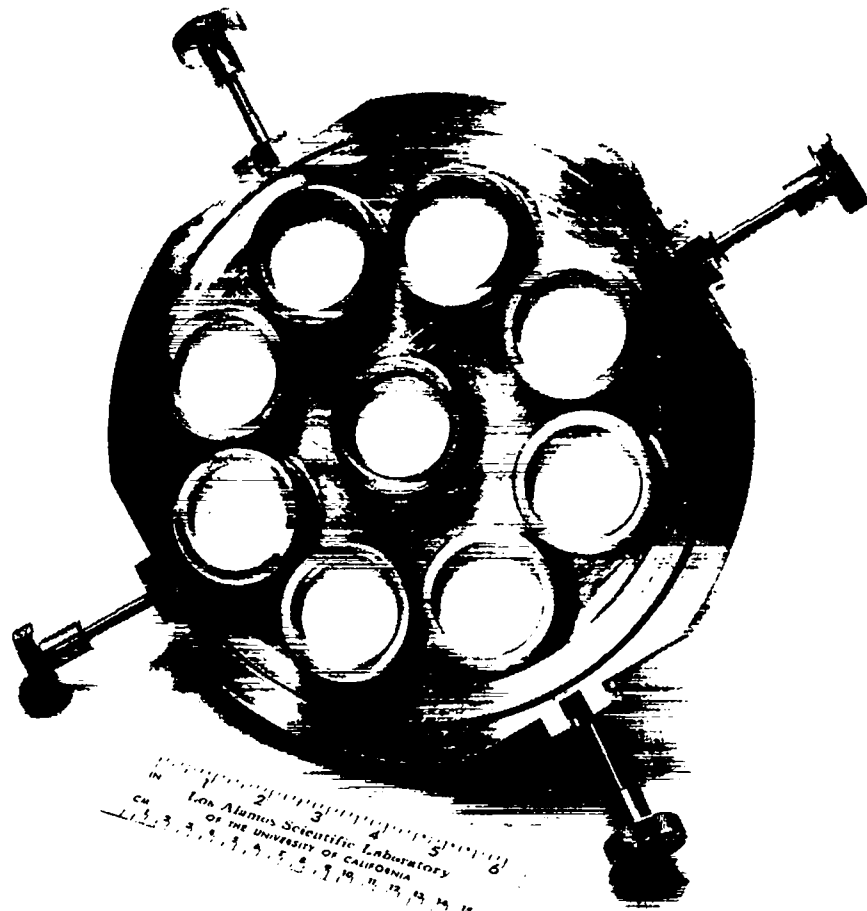


Fig. 12. Multiple Filter Holder

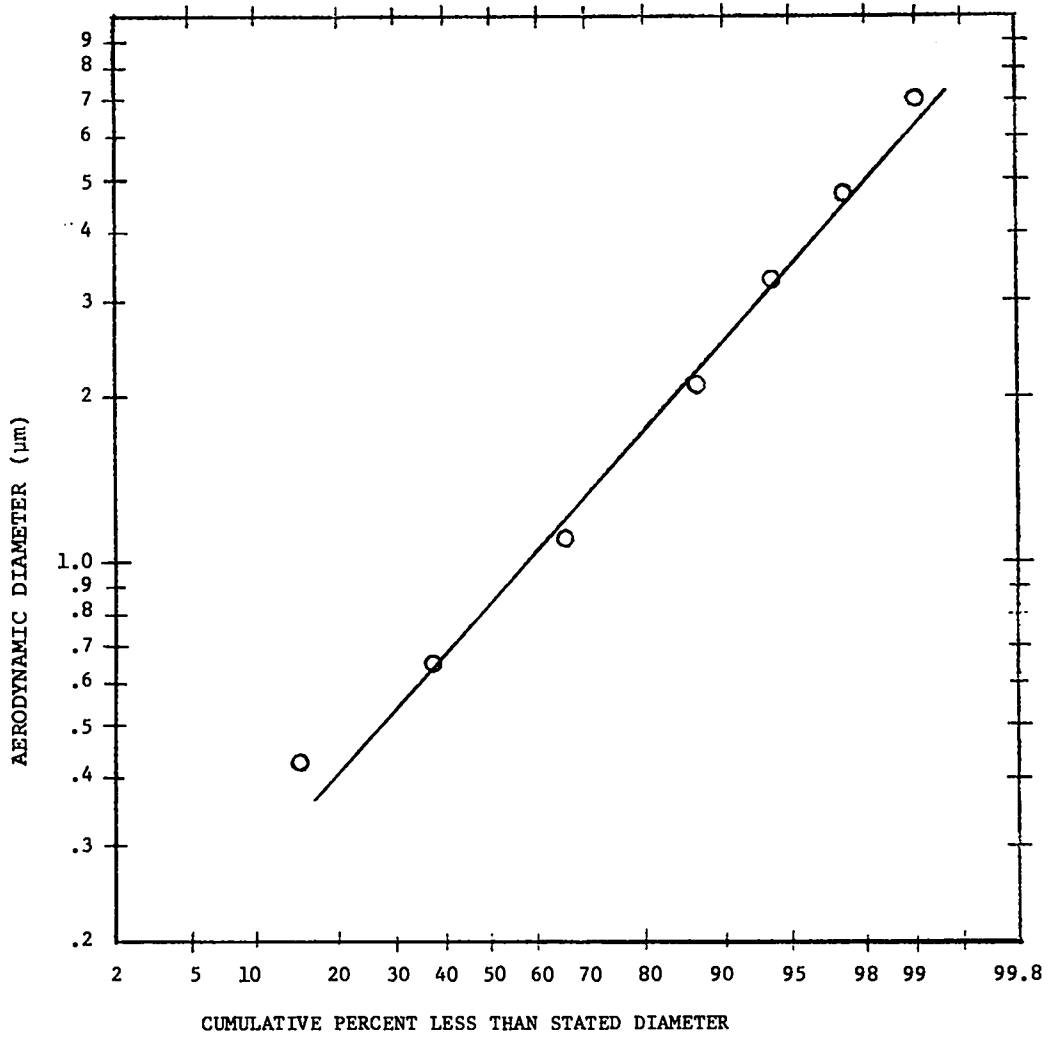


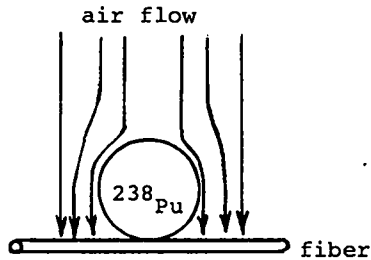
Fig. 13. Size Characteristics of Plutonium Aerosol From First Generating Test Run

APPENDIX
CALCULATIONS

September 19, 1972
Frank Harlow, T-3

Problem:

Spheres of highly radioactive material, which maintain high temperature because of continuing alpha decay, impinge, and collect on the fibers of a filter. Can they burn through the filter?



Simple Model: particle much larger than fiber diameter

Question: What will be the surface temperature of the particle?

$$\frac{\partial \rho b T}{\partial t} = V \cdot k \nabla T + S \quad (1)$$

Where ρ is density $g \text{ cm}^{-3}$

b is specific heat $\text{cal g}^{-1} \text{ } ^\circ\text{C}^{-1}$

T is temperature $^\circ\text{C}$

k is heat transfer coef. $\text{cal cm}^{-1} \text{ sec}^{-1} \text{ } ^\circ\text{C}^{-1}$

S is source energy per unit time per unit volume $\text{cal sec}^{-1} \text{ cm}^{-3}$

Under steady state conditions and using spherical coordinates, equation 1 reduces to:

$$\frac{1}{r^2} \frac{\partial}{\partial r} \left(r^2 k \frac{\partial T}{\partial r} \right) + S = 0 \quad (2)$$

$$r^2 k \frac{\partial T}{\partial r} = A - \frac{Sr^3}{3} \quad (3)$$

Due to spherical symmetry $\frac{\partial T}{\partial r} = 0$ at $r=0$, therefore $A = 0$, and

$$- k \frac{\partial T}{\partial r} = \frac{Sr}{3} = \text{heat flux as a function of } r \quad (4)$$

Heat flux at surface of particle ($r = R$) = $\frac{SR}{3}$

Integrating equation 4 $k T = A - \frac{Sr^2}{6} \quad (5)$

For Radiation Cooling Alone:

$$e a \left(T_s^4 - T_\infty^4 \right) = \frac{SR}{3}$$

where $a = 5.679 \times 10^{-5} \text{ erg cm}^{-2} \text{ sec}^{-1} \text{ } ^\circ\text{K}^{-4} \quad (6)$

T_s = surface temperature $^\circ\text{K}$

T_∞ = temperature at $r = \infty$

e = emissivity (assumed to be 1)

For Conductive Cooling:

Suppose the particle to be embedded in an infinite medium with heat transfer coefficient k_0 . At the boundary, T and $k \frac{\partial T}{\partial r}$ are considered to be continuous.

In the outer material where no heat is generated, $S = 0$. Equation 2 can be integrated to give:

$$r^2 k_0 \frac{\partial T}{\partial r} = \text{constant} = B \quad (7)$$

The constant B can be evaluated at $r = R$ by combining (7) and (4):

$$R^2 k_0 \frac{\partial T}{\partial r} = R^2 \left(-\frac{SR}{3} \right) = -\frac{SR^3}{3} \quad (7a)$$

Integrating (7a)

$$k_0 T = \frac{SR^3}{3r} + C \quad \text{where} \quad (8)$$

$$C = k_0 T_\infty \text{ at } r = \infty \quad \text{and}$$

$$k_0 T = k_0 T_\infty + \frac{SR^3}{3r} \quad (9)$$

Substituting T from (5) into (9), and letting $r = R$,

$$\frac{k_0}{k} \left(A - \frac{SR^2}{6} \right) = \frac{SR^2}{3} + k_0 T_\infty \quad \text{or} \quad (10)$$

$$A = k T_\infty + \frac{SR^2}{6} \left(1 + \frac{2k}{k_0} \right) \quad (11)$$

Substituting (11) into (5),

$$T = T_\infty + \frac{SR^2}{6k} \left(1 + \frac{2k}{k_0} \right) - \frac{Sr^2}{6k} \quad (12)$$

At $r = R$, $k = k_0$ and (12) reduced to:

$$T = T_\infty + \frac{SR^2}{3k_0} \quad (13)$$

Example of conductive heating:

$$k_0 = 5.48 \times 10^{-5} \text{ cal cm}^{-1} \text{sec}^{-1} \text{ } ^\circ\text{C}^{-1} \text{ for air at room temperature}$$

$$S = 0.567 \text{ watts gm}^{-1} = 1.36 \text{ cal sec}^{-1} \text{ cm}^{-3} = 5.67 \times 10^7 \text{ erg sec}^{-1} \text{ cm}^{-3}$$

$$T - T_\infty = \frac{1.36 R^2}{3 (5.48 \times 10^{-5})} = 8.3 \times 10^3 R^2$$

$$\text{For a particle with } R = 0.1 \text{ cm}$$

$$T - T_\infty = 83^\circ \text{ C}$$

$$\text{For } R = 2.5 \times 10^{-3} \text{ (or } 25 \text{ } \mu\text{m)}$$

$$T - T_\infty = 5.2 \times 10^{-2} \text{ } ^\circ\text{C}$$

Therefore, surface temperature rise due to conduction is negligible in very small particles.

Example of radiation heating:

From equation 6 :

$$1 \times 5.7 \times 10^{-5} \left(T_s^4 - T_\infty^4 \right) = 5.7 \times 10^7 \frac{R}{3}$$

$$T_s^4 \left(^\circ\text{K}^4 \right) = \frac{R}{3} \left(^\circ\text{K}^4 \right) \left(\text{cm}^{-1} \right) 10^{12} + T_\infty^4 \left(^\circ\text{K}^4 \right)$$

For $T_\infty = 300^\circ\text{K}$

$$T_s = \left(8.1 \times 10^9 + \frac{R}{3} 10^{12} \right)^{1/4}$$

$$= 300 \left(1 + \frac{10^3 R}{24.3} \right)^{1/4}$$

$$= 300 \left(1 + 41.2 R \right)^{1/4}$$

For Small R ($R < 10^{-2}$ cm),

$$T_s = 300^\circ \text{ k } (1 + 10.3R)$$

Thus, the surface temperature is not great for particles with $R \leq 10^{-2}$ cm. (100 μm)